Transportation Research Part C 111 (2020) 318–333

Contents lists available at ScienceDirect

Transportation Research Part C

journal homepage: www.elsevier.com/locate/trc

The Plugin Hybrid Electric Vehicle routing problem: A power-management strategy model

Sina Bahrami[a,*], Mehdi Nourinejad[b], Glareh Amirjamshidi[a], Matthew J. Roorda[a]

[a] Department of Civil & Mineral Engineering, University of Toronto, 35 St. George Street, Toronto, ON M5S 1A4, Canada
[b] Department of Civil Engineering, York University, 4700 Keele St, Toronto, ON M3J 1P3, Canada

ARTICLE INFO

Keywords:
Vehicle routing
PHEV
Branch-and-price
Charging
GVRP

ABSTRACT

This paper presents the Plugin Hybrid Electric Vehicle (PHEV) routing problem that finds the optimal set and sequence of customers visited by PHEVs to minimize total energy consumption. PHEVs use electricity and gasoline as their two energy sources. A power management model finds the optimal draw of power from the two sources along the vehicle's path. To solve the PHEVRP, we present an exact branch-and-price and a heuristic algorithm. We derive the complexity order of the algorithms and show that the heuristic becomes faster at larger battery capacities. We present a case study situated in the City of Toronto and show that the PHEVs use electricity in congested downtown regions and gasoline in free-flow conditions of highways.

1. Introduction

The transportation sector accounts for 70% of crude consumption and 28% of national greenhouse gas emissions in the U.S. and has great potential for decreasing petroleum dependency (US DOE, 2010). The Electrification Coalition, a not-for-profit group of business leaders that facilitate mass-scale deployment of electric vehicles, released a roadmap to examine the challenges of electrifying the transportation sector. By targeting consumer incentives and suggesting policies, the coalition plans to deploy 14 million grid-enabled light-duty vehicles in the U.S. by 2020 (Electrification Coalition, 2015). The coalition claims that commercial fleets have unique characteristics that make them strong candidates for electrification. Fleet owners are more willing than households to consider life cycle costs rather than upfront costs (Davis and Figliozzi, 2013), making them more inclined to switch to electric-drive vehicles. Moreover, fleet electrification can substantially aid the environment since medium and heavy-duty vehicles make up 4% of roadway vehicles (US FHWA, 2008), contributing to 19.2% of transportation-related greenhouse gas emissions.

Plugin Hybrid Electric Vehicles (PHEVs) are favorable in electrification because they fulfill emission regulations without sacrificing driving range. FedEx, a global courier delivery company, has converted 130 of its vehicles into plugin electric vehicles worldwide for daily operations that do not exceed 100 miles. For longer range deliveries, FedEx, working with Environmental Defense Fund and Eaton Corporation, delivers "the world's first street-ready hybrid truck." Similar to other vehicles, PHEVs visit a set of customers in their daily routes. This paper presents the PHEV routing model (PHEVRP) that finds the optimal customer visit sequence of each PHEV to minimize the total energy consumption.

PHEVs use electricity and gasoline as their two energy sources. A power management system finds the optimal power draw from the two sources along the vehicle's path. The energy consumption pattern is influenced by the driving cycle, which is a time-series

* Corresponding author.
E-mail addresses: sina.bahrami@mail.utoronto.ca (S. Bahrami), mehdi.nourinejad@lassonde.yorku.ca (M. Nourinejad), glareh.amirjamshidi@mail.utoronto.ca (G. Amirjamshidi), roordam@ecf.utoronto.ca (M.J. Roorda).

https://doi.org/10.1016/j.trc.2019.12.006
Received 5 May 2017; Received in revised form 10 December 2019; Accepted 14 December 2019

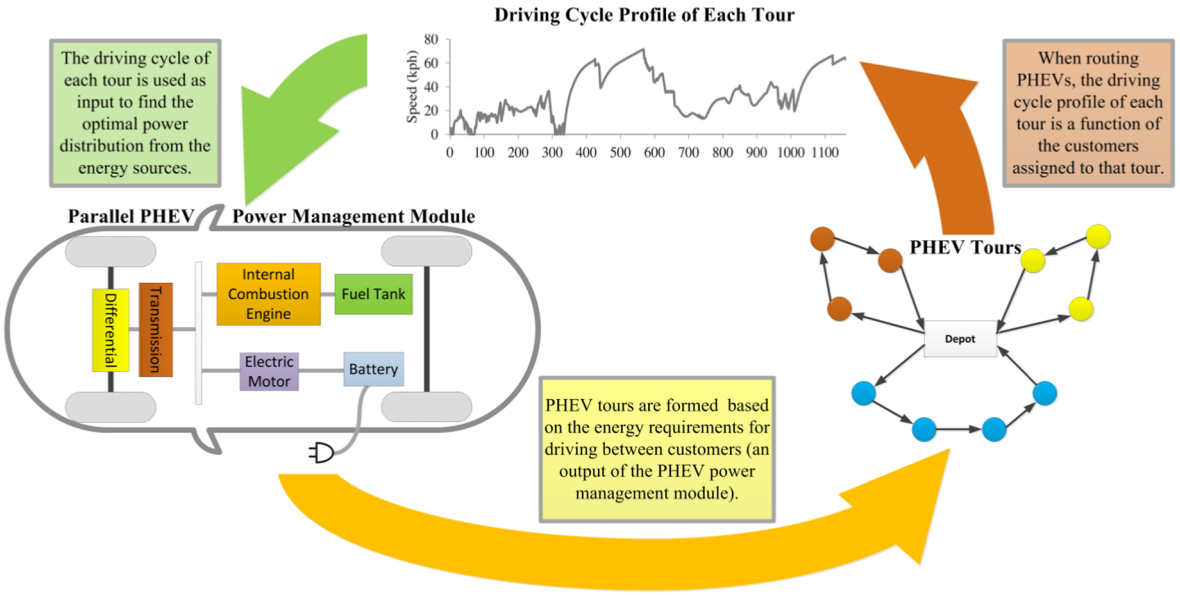

Fig. 1. Integration of the PHEV routing problem and the power management module.

profile of the vehicle's speed along its path; more energy is required as the vehicle accelerates. For a given driving cycle, the power management module finds the optimal power draw from the two energy sources (see the left green arrow in Fig. 1). In the vehicle routing problem (VRP), however, the driving cycle of each tour depends on the customer visit sequence of that tour, i.e., the driving cycle changes with respect to the customer visit sequence in each tour (right red arrow in Fig. 1). Hence, the power management module needs to have the customer visit sequence before drawing power from the two energy sources. When generating PHEV tours to create driving cycle profiles, the user-to-user (vertex-to-vertex) cost matrix needs to be appropriately defined. In the classical (VRP), the vertex-to-vertex cost is the distance or travel time between each two customers. In PHEV routing, however, this vertex-to-vertex cost is the total consumed energy from driving between users that depends on the outputs of the power management module (bottom yellow arrow in Fig. 1). Hence, PHEV routing and the power management module are related as illustrated in Fig. 1. The integration between the three components of Fig. 1 makes PHEV routing more complex than electric-vehicle routing and internal-combustion-engine vehicle routing.

The PHEV routing problem (PHEVRP) of this paper has two components: (i) vehicle routing to find the visit sequence, and (ii) power management optimization to draw energy from the two available energy sources. To solve the PHEVRP with both components, we present an exact branch-and-price and a heuristic algorithm. Our motivation for the heuristic algorithm is to solve problems that are too large for the exact method. We assess the performance of the two algorithms using numerical experiments on a set of benchmark examples. Results show that the two algorithms have similar performance when the battery is either small or large. In mid-range batteries, however, the exact method outperforms the heuristic as it finds a lower cost of routing at the expense of a longer computation time. The study provides several managerial insights. The model draws battery power in congested regions and uses gasoline in free-flow conditions of highways. The model generates the state-of-charge profile with different battery capacities and shows that they mostly consume all of their electricity at the end of their routes. The model allows us to capture the impact of chargers at designated customers on PHEV tours.

The paper is organized into the following sections. We present a review of the literature in Section 2. We formulate the model in Section 3 and present the power management module, a four-index routing model, a set partitioning formulation, and a branch-and-price algorithm for solving the set partitioning model. We present a heuristic algorithm for the PHEVRP in Section 4. We provide numerical experiments and a case study of a distribution company with PHEVs in the City of Toronto in Section 5. We present conclusions in Section 6.

2. Literature review

As there are currently only a few studies that explicitly consider the routing of PHEVs, we present a broader literature review of the green-VRP in Section 2.1, and we present the literature on PHEV power management strategies in Section 2.2.

2.1. Green vehicle routing

The green-VRP is extensively studied in the last decade (McKinnon et al., 2010; Dekker et al., 2012), however, only a few studies focus on electric vehicles and only one study investigates PHEV routing. Mancini (2017) presents a model for Hybrid Electric Vehicle routing where the vehicles can change propulsion modes (gasoline and electricity) along their route. Mancini (2017) presents a mixed

integer linear program for the problem and uses a Large Neighborhood Search based meta-heuristic algorithm to solve the problem. Our approach in this paper complements Mancini (2017) in the following ways. First, to obtain the optimal power split between the energy sources, we present a power management model for PHEVs. This model builds on the literature of PHEV power management strategies explained in Section 2.2. Second, we present an exact algorithm for the PHEVRP and we develop a customized heuristic model that is able to provide fast solutions. We derive the complexity order of the exact and the heuristic model and show that the heuristic becomes faster as the battery capacity of the PHEV becomes larger. Third, we derive insights on the optimal routing of PHEVs by graphically depicting the consumption patterns of the two power sources along the route of each PHEV.

The main feature that distinguishes PHEVRP from other VRPs is the presence of the driving range in the electric mode. Routing models that consider driving range are growing but still scarce. Bruglieri et al. (2019) formulate the VRP for alternative fuel vehicles while considering the driving range and the possibility of extending it by visiting a fueling station. The presented mixed integer linear program is strengthened by a set of logical inequalities, which only allow refueling between two consecutive customers if the remaining driving range is not enough to reach the next customer. Hence, the presented model by Bruglieri et al. (2019) outperforms the existing exact solution methods. Hiermann (2019) investigate the fleet composition of a VRP considering conventional vehicles, electric vehicles, and PHEVs. They assume that PHEVs can switch between the two energy sources at any given time, and their recharging time is proportional to the amount of charging. The problem is solved using a hybrid genetic algorithm. The numerical examples show that the operational cost of an optimal mixed fleet is lower than a homogeneous fleet. Conrad and Figliozzi (2011) present an electric-VRP model where electric vehicles are allowed to recharge at designated delivery locations. The problem assumes a fixed recharging time and considers the impact of the driving range and time windows on the optimal routing. Erdoğan and Miller-Hooks (2012) formulate a VRP that allows vehicles with limited range to refuel at select stations. They use two solution heuristics: a modified Clarke-Wright algorithm and a density-based clustering algorithm. The former algorithm pairs routes that either do not violate any constraints or only violate the range (distance) constraint that can be addressed by inserting a fuel station in the route. Gonçalves et al. (2011) model a VRP with pickup and delivery using a fleet of electric vehicles and conventional vehicles. The charging time of the electric vehicles is calculated using the total distance traveled and the capacity of the battery. The actual charger locations, however, are not incorporated in the model. Schneider et al. (2014) present an electric-VRP with time windows and charging stations. While similar to Conrad and Figliozzi (2011) in terms of problem definition, the authors present a new heuristic solution algorithm that hybridizes a neighborhood search algorithm with a Tabu Search algorithm. The model is then tested on benchmark instances to show the benefits of hybridization. Abdallah (2013) presents a Tabu Search model for routing PHEVs in realistic size instances. The model, however, disregards the role of the power management module and assumes a linear relationship between electricity and gasoline consumption.

Although the green-VRP literature faces a shortage of research on electric vehicle routing, reasonable investigations are dedicated to the VRP with energy or emissions minimization. The emissions VRP was first introduced by Figliozzi (2010) where the capacitated-VRP was modified to include the driving speed and departure time as two decision variables to minimize emissions. Bektas and Laporte (2011) introduce the pollution routing problem to minimize a cost function composed of emissions, fuel consumption, and driver costs. Emissions and fuel consumption are functions of vehicle speed, payload, grade, and vehicle curb weight. Computational studies on small-size examples show that although labor costs are dominant, it is still possible to reduce total emissions. Demir et al. (2012) develop an adaptive large neighborhood search algorithm for the pollution routing problem. Demir et al. (2014) introduce the bi-objective population routing problem to minimize fuel consumption and driving time using an adaptive large neighborhood search algorithm. Franceschetti et al. (2013) present the time-dependent population routing problem. Jabali et al. (2012) present a Tabu Search algorithm to solve a VRP for minimizing emissions when the travel times are time-dependent. Using several computational experiments, Jabali et al. (2012) conclude that reducing emissions leads to reducing costs as the two are correlated. Kwon et al. (2013) and Kopfer et al. (2014) consider the influence of a heterogeneous fleet on emissions. Koc et al. (2014) propose a fleet composition problem to minimize the sum of vehicle fixed costs and pollution routing costs. Deflorio and Castello (2017) study the impacts of charging while driving in freight delivery service vehicles.

The PHEVRP is distinguished from the green-VRP and electric-VRP literature in the following ways. While EVs only use electricity to travel, PHEVs have two sources of energy with different rates of emission. Hence, it is imperative to use the power management module to optimally distribute power between the two energy sources. Moreover, electric-VRP models are prominently cost minimizers (e.g., minimizing the total vehicle travel time) whereas our model minimizes the total energy consumption. Particularly, the objective function is to minimize the total gasoline consumption as is advocated in PHEV power management studies such as He et al. (2012).

2.2. PHEV power management strategy

Power management strategies are optimization models that distribute power between the two energy sources to propel the wheels. The two main PHEV power management strategies are “charge sustaining/charge depletion” and “blended” (Raykin et al., 2012). In the former, when in the charge-depleting mode, the PHEV uses the battery until the state-of-charge reaches a predefined limit. Then, by shifting to the charge sustaining mode, the PHEV maintains a relatively constant state-of-charge. The blended mode, however, involves an even depletion of the battery throughout the trip. Thus, the blended is better because it has higher flexibility in switching between the two power sources whereas the charge-sustaining/charge-depletion mode does not. This paper focuses on the blended mode due to its superiority to the charge sustaining/charge depletion mode (Zhang et al., 2009).

Optimization of PHEV power management is either offline or online (Sinoquet et al., 2011; Ribau et al., 2014a; Qi et al., 2019; Yao and Moaawd, 2019). In offline optimization, the driving cycle is known a priori. For practical implementation, however, online

optimization is required where the driving cycle is uncertain. Although offline optimization poses some practical restrictions, it is used as a benchmark to assess the quality of any realistic but suboptimal online controller (Ribau et al., 2014b). We use an offline model in solving the PHEVRP. Offline power management problems are solved using global optimization techniques that are further divided into static (Oh et al., 2007), dynamic (Chen et al., 2014), and other methods including stochastic control (Kolmanovsky et al., 2008) and nonlinear regulation (Sampathnarayanan et al., 2014). Zhang et al. (2015) present a thorough survey of these methods. Among these surveyed methods, dynamic programming is the most popular and heavily used strategy. We use a modified dynamic program as the optimal power management strategy. The modification involves running the dynamic program multiple times instead of only once as is done in the literature. The details of the presented dynamic program are elaborated in Section 3.

3. The Plugin Hybrid Electric Vehicle routing problem

This section is organized into the following. Section 3.1 describes the power management problem of a single vehicle. Sections 3.2 and 3.3 present the four-index formulation and set partitioning formulation of PHEVRP problem for a fixed fleet size. Finally, Section 3.4 presents a branch-and-price algorithm for the set partitioning problem.

3.1. Power management module

Let $G = \{V, A\}$ be a complete directed graph with vertex set $V = \{0, 1, 2, \cdots, v\}$, where vertex 0 is the depot and $V_0 = \{1, 2, \cdots, v\}$ is the set of v customers. For every $(i, j) \in A$, let d_{ij} be the distance from vertex i to vertex j discretized into $|K_{ij}|$ equal-length segments represented by the set $K_{ij} = \{1, 2, \cdots, k, \cdots, |K_{ij}|\}$. The required wheel power when traveling segment k of arc (i, j) is denoted by P_{ij}^k, which is obtained from the driving cycle profile (i.e., the speed profile of the vehicle along its route). Let $\widehat{P}_{ij}^k$ and $\breve{P}_{ij}^k$, $\forall\ (i, j) \in A$, $\forall\ k \in K_{ij}$, be decision variables that denote the electric motor and the gasoline engine power at segment k of arc (i, j), respectively. The power management module finds $\widehat{P}_{ij}^k$ and $\breve{P}_{ij}^k$ to meet the required wheel power such that $P_{ij}^k = \widehat{P}_{ij}^k + \breve{P}_{ij}^k$. We discretize the battery capacity into $|M|$ charge levels where the levels are represented by the Set $M = \{1, 2, \cdots, m, \cdots, |M|\}$. The charge level $m = 1$ and $m = |M|$ indicate that the vehicle has an empty and a full state-of-charge (SOC), respectively. Fig. 2 presents a schematic of the Set K_{ij}, the charge levels M, the driving cycle, and the required power P_{ij}^k for two customers i and j. In Fig. 2, we note that the driving cycles are highly random and subject to traffic conditions. However, the required power profile is aggregate (in terms of changes with respect to time), and more robust. Although we have variations in the driving cycle, the aggregate required power function is less uncertain.

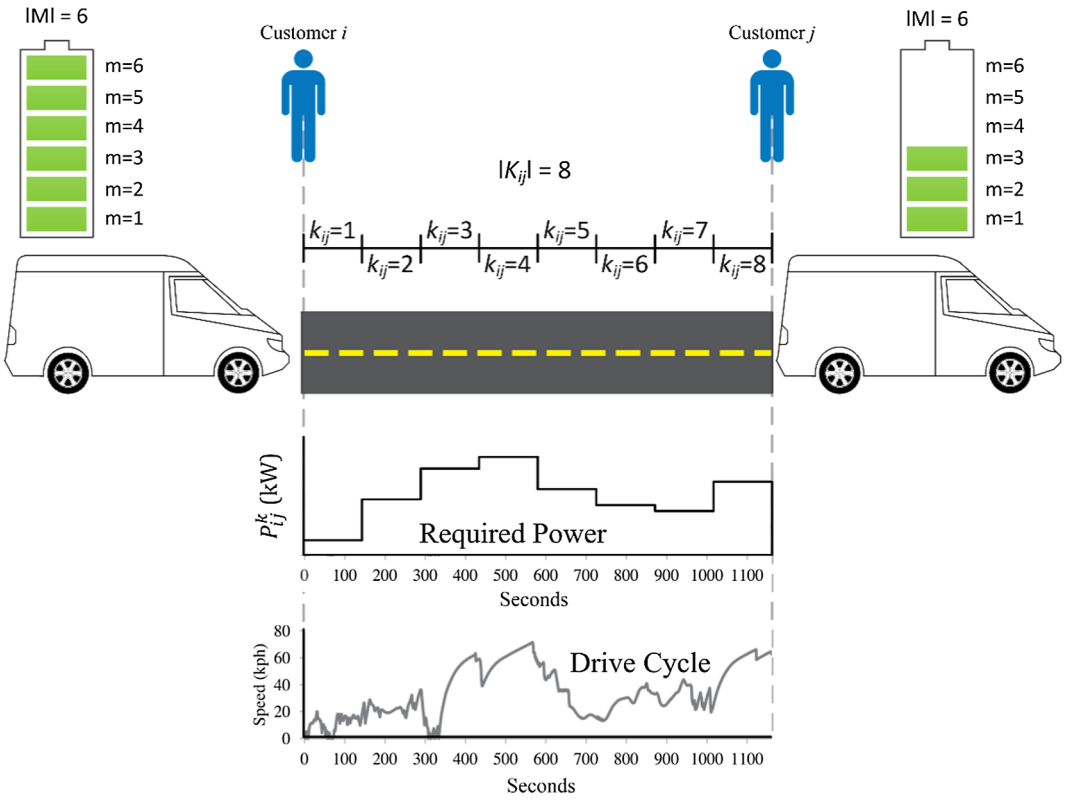

Fig. 2. Power management states when traveling from customer i to customer j.

Let $S_i = \{s_i^m, \forall\, m \in M\}$ be a vector where s_i^m is a binary variable equal to 1, and otherwise 0, when the vehicle is at charge-level $m \in M$ upon leaving customer $i \in V_0$. The state-space (i, m) is appropriate when the set of nodes to be visited and sequence are predetermined. In Fig. 2, we have $s_i^6 = 1$ because the vehicle leaves customer i with charge-level $m = 6$. Let $S_{ij}^k = \{s_{ij}^{km}, \forall\, m \in M\}$ be the state vector at segment $k \in K_{ij}$ of arc $(i, j) \in A$ where s_{ij}^{km} is a binary variable equal to 1, and otherwise 0, when the vehicle is at SOC level m at segment k. The state evolution equation is formulated using the function ϕ as:

$$S_{ij}^{k+1} = \phi\left(S_{ij}^k, \widehat{P}_{ij}^k, \breve{P}_{ij}^k\right), \quad \forall\, (i, j) \in A,\ k \in K_{ij} \tag{1}$$

which shows that the SOC at segment $k + 1$ of arc (i, j) depends on its SOC at segment k and the action $\left(\widehat{P}_{ij}^k, \breve{P}_{ij}^k\right)$ taken at segment k. The objective of the power management module is to find the optimal power distribution between the two energy sources, i.e., $\left(\widehat{P}_{ij}^k, \breve{P}_{ij}^k\right)$, to minimize gasoline consumption while justifying Eq. (1) and other technical constraints. Let $\psi\left(S_{ij}^k, \widehat{P}_{ij}^k, \breve{P}_{ij}^k\right)$ be the gasoline consumption on segment $k \in K_{ij}$ of arc (i, j), which is a function of the charge state S_{ij}^k and the power distribution strategy $\left(\widehat{P}_{ij}^k, \breve{P}_{ij}^k\right)$.

We formulate the power management module as the following optimization model:

$$\pi_{ij} = min \sum_{k=1:K_{ij}} \psi\left(S_{ij}^k, \widehat{P}_{ij}^k, \breve{P}_{ij}^k\right) \tag{2}$$

subject to Eq. (1) and

$$S_{ij}^1 = S_i \tag{3}$$

$$S_{ij}^{|K_{ij}|} = S_j, \tag{4}$$

where S_i and S_j are input vectors to specify the initial and final SOC, respectively. As an example, in Fig. 2, we have $S_i = \{0, 0, 0, 0, 0, 1\}$ and $S_j = \{0, 0, 1, 0, 0, 0\}$. The objective function in Eq. (2) is subject to technical constraints bounding the allowable speed and torque of the engine and the motor. We assume that the technical constraints are justified when solving the following dynamic program. According to Bellman's principles, the optimal energy management strategy solves sub-problems of the optimization backwards from the final SOC condition $S_{ij}^k = S_j$. Hence, the sub-problem for the $|K_{ij}|^{th}$ step is to minimize

$$\pi_{ij}^k = \min\{\psi(S_{ij}^k, \widehat{P}_{ij}^k, \breve{P}_{ij}^k)\}, \quad \forall\, k = |K_{ij}| \tag{5}$$

where π_{ij}^k is the cost-to-go function at segment k. Because we are looking at the final step, Eq. (5) is also the one-step cost of step $|K_{ij}|$, where $|K_{ij}|$ is the cardinality of Set K_{ij}. For all other segments of arc (i, j) the sub-problem is to minimize

$$\pi_{ij}^k = min\{\psi(S_{ij}^k, \widehat{P}_{ij}^k, \breve{P}_{ij}^k) + \pi_{ij}^{k+1}\} \quad \forall\, k = 1{:}\ |K_{ij}| - 1 \tag{6}$$

In conventional power management models for household trips, S_j in Eq. (4) is set to the lowest SOC because it is assumed that vertex j is the home location where the vehicle can be parked overnight and recharged. In vehicle routing, however, the vehicle consecutively visits a set of customers. Hence, it is not logical to set S_j to the lowest SOC because it would mean that the vehicle has no remaining charge when traveling to the next customer. Thus, we run the dynamic program for all feasible vectors $S_i = \{s_i^m\}$ and $S_j = \{s_j^n\}$ as inputs (see Eqs. (3) and (4)). From all feasible charge level m, $n \in M$, the VRP chooses one pair of (m, n) when traveling arc (i, j). We note that not all m, $n \in M$ are feasible for a given arc (i, j). For instance, having $n > m$ indicates an increase in the SOC of the vehicle that traverses arc (i, j), which is illogical unless a charger is available at vertex $j \in V_0$.

Let Ω_{ij} be the set of all feasible pairs (m, n) for traversing arc (i, j) and let μ_{ij}^{mn} be the total gasoline consumption when the vehicle leaves node i with SOC level m and arrives at node j with SOC level n. We use dynamic programming to generate the Set Ω_{ij} for a given (i, j) along with μ_{ij}^{mn} of each pair (m, n) in the set Ω_{ij}.

We now explain the impact of chargers at customer locations. Longer service times and faster chargers increase the SOC. Let $\widehat{m}_i$ denote the increase in the number of charge levels of a vehicle that visits customer i with a charger. To incorporate charging, the Set Ω_{ij} is revised so that for each $(m, n) \in \Omega_{ij}$, we have:

$$(m, n) \rightarrow (m, n + \widehat{m}_j): \quad if \quad n + \widehat{m}_j < |M| \tag{7a}$$

$$(m, n) \rightarrow (m, |M|): \quad if \quad n + \widehat{m}_j \geq |M|. \tag{7b}$$

In Eq. (7a), the vehicle does not surpass its battery capacity after charging at j. Hence, the vehicle arrives at vertex j with SOC level n and it leaves vertex j at SOC level $n + \widehat{m}_j$. In Eq. (7b), however, the SOC would surpass the battery capacity if charged at vertex j. Hence, the vehicle's battery is at full capacity $|M|$ upon leaving node j. The charging model assumes a fixed visiting duration at each vertex j. Relaxing this assumption may create better charging opportunities but would require new decision variables in the model, which is outside the scope of our study.

3.2. The four-index PHEVRP

We present the four-index arc-charge PHEVRP where the binary decision variable x_{ij}^{mn} is 1, and otherwise 0, if a vehicle leaves vertex $i \in V$ with SOC level $m \in M$ and arrives at vertex $j \in V$ with SOC level $n \in M$. The concept of the four-index arc-charge PHEVRP comes from extending the three-index arc-load capacitated vehicle routing model of Uchoa (2011).

The arc-charge formulation of the PHEVRP with fleet size F is as follows:

$$min \sum_{(i,j)\in A} \sum_{m\in M} \sum_{n\in N} \mu_{ij}^{mn} x_{ij}^{mn} \tag{8}$$

s.t.

$$\sum_{j\in V\setminus\{i\}} \sum_{n\in M} x_{ij}^{mn} = 1 \quad \forall\, i \in V_0,\, m \in M \tag{9}$$

$$\sum_{j\in V\setminus\{i\}} \sum_{m\in M} x_{ji}^{mn} - \sum_{j\in V\setminus\{i\}} \sum_{m\in M} x_{ij}^{nm} = 0 \quad \forall\, i \in V_0,\, \forall\, n \in M \tag{10}$$

$$\sum_{i\in V_0} \sum_{m\in M} \sum_{n\in M} x_{i0}^{mn} = F \tag{11}$$

$$\sum_{i\in V_0} \sum_{n\in M} x_{0i}^{mn} = F \quad m = |M| \tag{12}$$

$$x_{ij}^{mn} \in \{0, 1\} \quad \forall\, (i, j) \in A,\, \forall\, m, n \in M \tag{13}$$

The objective function in Eq. (8) minimizes the total gasoline consumption. Constraints (9) ensure that each customer is visited exactly once. Constraints (10) represent the charge balance at each customer $\forall\, i \in V_0$. Constraint (11) ensures that a total of F vehicles are used. Constraints (12) ensure that vehicles leave the depot with a full SOC, i.e. $m = |M|$. Constraints (13) are integrality constraints.

3.3. A set partitioning formulation

There are various examples of the set portioning formulation in capacitated-VRPs (Fukasawa et al., 2006; Eksioglu et al., 2009; Pillac et al., 2013). Motivated by these studies, a set partitioning formulation for the PHEVRP is presented here based on the concept of q-routes. We define a q-route as a walk $i_0 i_1 i_2 \cdots i_q i_0$ where $i_1 i_2 \cdots i_l \in V_0$, $i_0 = 0$ is the depot, and all traversed arcs are within the feasibility set Ω_{ij}. For the set of q-routes that are 2-cycle free (i.e. routes with no cycles $i \to j \to i$), we denote the binary variable z_r to indicate whether the q-route r is chosen or not. Let a_{ijr} denote the number of times that arc (i, j) is visited in route r; let a_{ir} denote the number of times that customer i is visited in route r such that $a_{ir} = \sum_j a_{ijr}$; let μ_r be the fuel consumption of route r. The set of all 2-cycle-free q-routes is denoted by R.

The set partitioning formulation of the PHEVRP is as follows:

$$min \sum_{r\in R} \mu_r z_r \tag{14}$$

s.t.

$$\sum_{r\in R} a_{ir} z_r = 1 \quad \forall\, i \in V_0 \tag{15}$$

$$\sum_{r\in R} z_r = F \tag{16}$$

$$\sum_{r\in R} \beta_t z_r \geq \sigma_t \quad \forall\, t \in T \tag{17}$$

$$z_r \in \{0, 1\}, \quad \forall\, r \in R \tag{18}$$

where the objective function in Eq. (14) minimizes the total gasoline consumption. Constraints (15) ensure that each customer is visited exactly once. Constraints (16) ensure that F vehicles are used. Constraints (17) impose a set T of branch and bound constraints that are explained in Section 3.4. We note that Constraint (16) may be eliminated as it can be included in the set of Constraints in (17). Constraints (18) ensure integrality of the decision variables. We solve the linear programming (LP) relaxation of (14)–(18) by column generation since there is an exponential number of decision variables. We obtain the LP relaxation, called the Dantzig-Wolfe Master (DWM) problem, by relaxing Constraints (18) and replacing them with $z_r \geq 0$, $\forall\, r \in R$.

3.4. The branch-and-price algorithm

We present a branch-and-price (BP) algorithm for the set partitioning problem. The BP algorithm builds on a branch-and-bound

tree, where we solve the DWM problem using column generation at each node of the tree. We focus on describing the details of the pricing problem as all other components of the BP algorithm are similar to the existing models in the literature (Toth and Vigo, 2014) and hence are only briefly mentioned here.

3.4.1. The pricing problem

For a given solution of the primal LP of the DWM problem, we solve the pricing problem find a new route (column) with a negative reduced cost. In the capacitated VRP, the pricing problem involves finding a minimum cost 2-cycle-free q-route in graph G where the cost of each arc is obtained from the optimal dual variables of the restricted DWM problem, and the cost of each q-route is the sum of the cost of the arcs (comprised of the dual variables) in that q-route. Let λ_i and τ^t, $\forall\, i \in V$, $t \in T$ be the optimal dual variables of Constraints (15), and (17), respectively. We do not individually consider Constraint (16) because it can be included in the set of Constraints (17). We let $\lambda_0 = 0$ for the depot. The pricing problem is now formulated as:

$$\min_{r\in R} \overline{\mu}_r = \mu_r - \sum_{i\in V} \lambda_i a_{ir} - \sum\nolimits_{t\in T} \tau^t \sum\nolimits_{(i,j)} \alpha_{ij}^t a_{ijr}. \tag{19}$$

The challenge in applying the conventional pricing problems to the PHEVRP is the presence of multiple energy management strategies between each two vertices. Hence, the concept of dual variable arc costs does not directly apply in the PHEVRP as it does in the capacitated-VRP where there is only one route between each two vertices. In addressing a similar challenge, Fukasawa et al. (2015) solve the pricing problem as a shortest q-route problem over a multigraph. A similar modified methodology is applied here for the PHEVRP. We now show in three steps that the pricing problem (19) can be reformulated as a shortest path q-route problem over a multigraph.

First, for a given q-route r, let a_{ijr}^{mn} be a binary index equal to 1, and otherwise 0, if the q-route r traverses arc (i, j) while leaving vertex i with SOC level m and arriving at vertex j with SOC level n. The q-route r cost μ_r is defined as:

$$\mu_r = \sum_{(i,j)\in A} \sum_{(m,n)\in\Omega_{ij}} \mu_{ij}^{mn} a_{ijr}^{mn}. \tag{20}$$

Second, the term $\sum_{i\in V} \lambda_i a_{ir}$ in Eq. (19) computes the cumulative $\lambda_i^{'}s$ for q-route r. When a customer $i \in V_0$ is visited, two arcs are traversed adjacent to customer i, one entering and one leaving the customer. Given that $a_{ijr} = \sum_{(m,n)\in\Omega_{ij}} a_{ijr}^{mn}$, we have:

$$\sum_{i\in V} \lambda_i a_{ir} = \sum_{(i,j)\in A} \left(\frac{\lambda_i}{2} + \frac{\lambda_j}{2}\right) a_{ijr} = \sum_{(i,j)\in A} \sum_{(m,n)\in\Omega_{ij}} \left(\frac{\lambda_i}{2} + \frac{\lambda_j}{2}\right) a_{ijr}^{mn}. \tag{21}$$

Third, by substituting Eqs. (20) and (21) into Eq. (19), we have:

$$\overline{\mu}_r = \sum_{(i,j)\in A} \sum_{(m,n)\in\Omega_{ij}} \mu_{ij}^{mn} a_{ijr}^{mn} - \sum_{(i,j)\in A} \sum_{(m,n)\in\Omega_{ij}} \left(\frac{\lambda_i}{2} + \frac{\lambda_j}{2}\right) a_{ijr}^{mn} - \sum\nolimits_{t\in T} \sum_{(i,j)\in A} \sum_{(m,n)\in\Omega_{ij}} \tau^t \alpha_{ij}^t a_{ijr}^{mn}, \tag{22}$$

which can be rewritten as

$$\overline{\mu}_r = \sum_{(i,j)\in A} \sum_{(m,n)\in\Omega_{ij}} \left[\mu_{ij}^{mn} - \left(\frac{\lambda_i}{2} + \frac{\lambda_j}{2}\right) - \sum\nolimits_{t\in T} \tau^t \alpha_{ij}^t\right] a_{ijr}^{mn} = \sum_{(i,j)\in A} \sum_{(m,n)\in\Omega_{ij}^{mn}} \overline{\mu}_{ij}^{mn} a_{ijr}^{mn}, \tag{23}$$

where $\overline{\mu}_{ij}^{mn} = \mu_{ij}^{mn} - \left(\frac{\lambda_i}{2} + \frac{\lambda_j}{2}\right) - \sum_{t\in T} \tau^t \alpha_{ij}^t$. Hence, the pricing problem can be redefined as:

$$\min_{r\in R} \overline{\mu}_r = \sum_{(i,j)\in A} \sum_{(m,n)\in\Omega_{ij}} \overline{\mu}_{ij}^{mn} a_{ijr}^{mn}, \tag{24}$$

which is equivalent to solving a shortest 2-cycle-free q-route over a multigraph $(V, \overline{A})$ where the arc set $\overline{A}$ includes Ω_{ij} parallel arcs between each two vertices $i, j \in V_0$. We use a dynamic programming algorithm to solve the pricing problem in pseudo-polynomial time for 2-cycle-free q-routes. Let L be a $|M| \times v$ matrix where each element $L(m, w)$ represents the gasoline consumption of the 2-cycle-free walk reaching customer w with SOC level m, let $vr(m, w)$ be the last vertex before reaching w with SOC level m on that q-route, and let $cr(m, w)$ be the SOC before reaching w with SOC level m on that q-route. Let $\mathscr{L}_w = \min_{(m,n)\in\Omega_{w0}} \{L(m, w) + \overline{\mu}_{w0}^{mn}\}$ be the minimum gasoline consumption of the 2-cycle free feasible q-route whose last visited vertex is w with SOC level m before heading back to the depot with SOC level n and let $\varphi_w = \arg\min_{(m,n)\in\Omega_{w0}} \{L(m, w) + \overline{\mu}_{w0}^{mn}\}$.

Algorithm 1. *Pricing algorithm for* 2*-cycle-free feasible q-routes in* (V, A_M)

Inputs: $\overline{\mu}_{ij}^{mn}$, $\forall\, (i, j) \in A$, $(m, n) \in \Omega_{ij}$

Outputs: $\mathscr{L}_w$, φ_w, vr, cr

Step 1: *initialize*
Step 2: *create v one-customer routes*
For $w = 1$ *to* v
  For$n = 1$ *to* $|M|$

Inputs: $\bar{\mu}_{ij}^{mn}, \forall\ (i, j) \in A, (m, n) \in \Omega_{ij}$
Outputs: $\mathscr{L}_w, \varphi_w, vr, cr$

```
    If (|M|, n) ∈ Ω_0w
      L(n, w) ← μ̄_0w^{|M| n}
      vr(n, w) ← 0
      cr(n, w) ← |M|
      End if
    End for
    End for
Step 3: construct L, vr, and cr
For u = 1 to v
  For w = 1 to v
    For m = 1 to |M|
      For n = 1 to |M|
        If (m, n) ∈ Ω_uw and w ≠ u and w ≠ vr(m, u) and L(m, u) + μ̄_uw^mn < L(n, w)
          L(n, w) ← L(m, u) + μ̄_uw^mn
          vr(n, w) ← u
          cr(n, w) ← m
          End if
        End for
      End for
  End for
Step 4: return final outputs
  ℒ_w = min_{(m,n)∈Ω_w0} {L(m, w) + μ̄_w0^mn}
  φ_w = arg min_{(m,n)∈Ω_w0} {L(m, w) + μ̄_w0^mn}
```

The pricing problem is solved in $O(|M|^2v^2)$ time. Although the pricing problem can be solved using s-cycle-free q-route (where $s \geq 3$) to provide tighter LP bounds, the increased computation time and memory storage do not justify the benefits. All 2-cycle-free q-routes with $\mathscr{L}_w < 0$, where w is the last visited customer of that q-route, are added to the DWM problem as new columns. The visited customers and the SOC on these q-routes are retrieved by stepping backwards from customer w using matrices vr and cr in the following way. Starting with customer w, the second last vertex (before returning to the depot) is $vr(\varphi_w, w)$ who was visited at SOC level $cr(\varphi_w, w)$. The tracking continues until we reach the starting point (depot).

3.4.2. Branching rules, node selection, and primal bounds

After solving the pricing problem, the branch-and-bound algorithm is solved with the newly generated columns. The applied branching rule is "Most Infeasible Branching". The initial solution of the primal is obtained by solving the four-index formulation (problem (8)–(13)) until a feasible solution is obtained. The node selection strategy in the branch-and-bound is based on a "depth first" search. From the branch-and-bound process we obtain the Sets T, α_{ij}^t, and σ^t.

4. Heuristic model: route first, distribute second

The heuristic model has the following steps. We first assign one cost to each arc of the network. This cost is the cost of traveling the arc in all-gasoline mode without using any electricity. By assigning only one cost to each arc, we limit the size of the power-management strategy, i.e., Ω_{ij}, to only one strategy (per arc (i, j)), which is to drive in all-gasoline mode. The optimal tour can be obtained using any VRP algorithm since each arc has a single associated cost. The solution of the VRP is the tour assigned to each vehicle in the fleet. This completes the first stage of the heuristic algorithm that we call "route-first".

By solving the "route-first" stage, we have assigned one tour to each vehicle in the fleet. In the second stage, called "distribute-second", we decide how to distribute power from the two energy sources. This is done by taking each vehicle-tour and running the dynamic program of Section 3.1 to find the optimal power distribution between the two energy sources along the vehicle's path. In a way, the two-stage heuristic algorithm decouples the routing from the power management module that in turn reduces the complexity of the problem and allows for faster solutions. The reduction in the complexity depends on the battery capacity. As an example, consider a graph with v nodes and a battery capacity of size $|M|$. While the exact pricing method is solved in order $O(|M|^2v^2)$, the heuristic can be solved in $O(v^2)$. Hence, the savings in the solving the "route-first" component is at least of the order $O(|M|^2)$. Nevertheless, the order of the "distribute-second" component of the heuristic also has to be considered for a more accurate comparison of the two algorithms.

5. Numerical experiments

We perform numerical experiments to derive insights from the model and to test the model's applicability in real-life instances. The first set of tests is performed on a circular network with the depot located at the center and the customers located on the circumference of the circle. The second set of tests evaluates the performance of the exact model and the heuristic and the third test

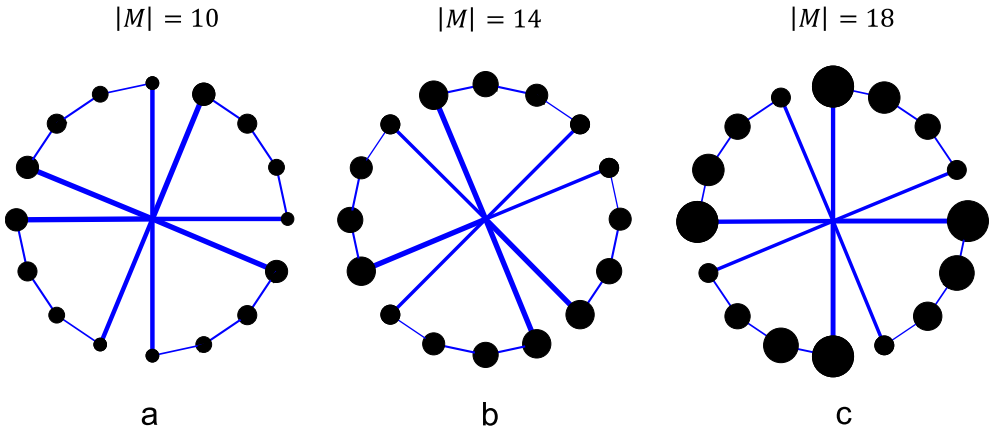

Fig. 3. Graphical representation of PHEVRP for different battery capacities in circular networks.

captures the impact of charging in a real-life network of the City of Toronto.

5.1. A circular network

Consider a circular network where the depot is in the center and the customers are on the circumference. We have 4 vehicles and 16 customers. The routing scheme for this circular network is presented in Fig. 3 for four different battery capacities. As the vehicles drive along their path, their remaining electric-charge (on the battery) decreases to the point where they have no remaining charge when they return to the depot. The size of the black nodes in Fig. 3 represents the vehicle's SOC that decreases as the vehicle proceeds along its path. The vehicles have the lowest SOC when they return to the depot. The thickness of the blue lines represents the intensity of gasoline consumption along each arc. As shown, the highest gasoline consumption occurs on arcs that emanate from and terminate at the depot. This happens because of the long line-haul distance between the depot and the customers in circular networks.

We analyze the impact of the battery capacity on the PHEVRP. We consider six different battery capacities and assume that the vehicles can drive in five different driving modes. Mode 1 is all-electric and Mode 5 is all-gasoline. The other modes (Mode 2, 3, and 4), use a mix of gasoline and electricity. In total, there are 20 edges in the network (see Fig. 3) because there are four vehicles and 16 customers. We test the driving frequency of the vehicles in each of the 5 modes along the 20 edges of the network. The results of the mode frequencies along the two edges are depicted in Fig. 4. When the electric-range is low (6 km), the vehicles drive only in Mode 5 (all-gasoline) along all the 20 edges of the network (see the darkest bar in Fig. 4). However, when the electric range is high (26 km), the vehicles drive only in Mode 1 (all-electric) along all the 20 edges of the network (see the lightest bar in Fig. 4). For all other electric ranges, the vehicles use a mix of all the modes to minimize their total gasoline consumption without violating the driving range.

We also present the total gasoline and electric consumption at different battery capacities in Fig. 5. As the battery capacity increases, the vehicles use more electricity along their path. Hence, the total electricity consumption goes up with the electric driving range. This indicates that the vehicles can reduce their gasoline consumption because of their higher electricity usage. Hence, the total gasoline consumption goes down as the driving range increases as shown in Fig. 5.

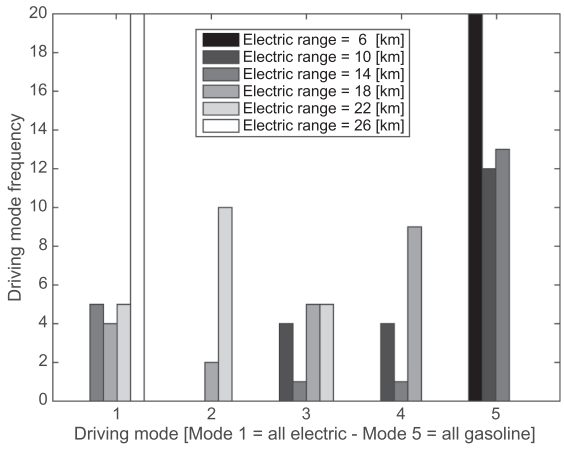

Fig. 4. Frequency of the five modes in a circular network with 20 edges.

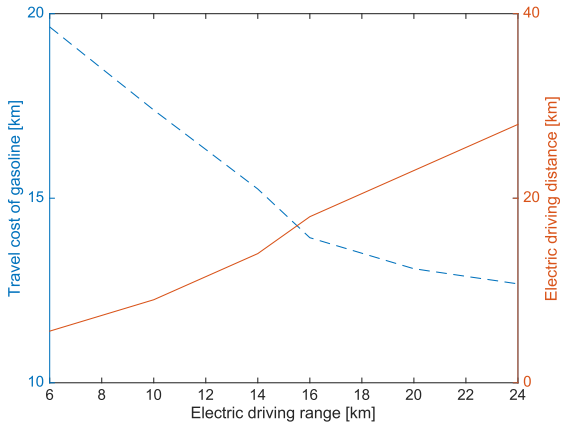

Fig. 5. Gasoline and electricity consumption in a circular network with 20 edges and 4 vehicles.

We analyze the sensitivity of the model with respect to different number of vehicles. Four instances are presented in Fig. 6 with $F = 2, 3, 4, 5$ and four customers per vehicles. In all instances, it is evident that the vehicles use their electric power in the beginning of their path. Towards the end of the path, however, the vehicles consume more gasoline as their SOC reaches zero. This confirms earlier findings of power management strategy models. This higher gasoline usage is depicted in the thickness of the blue lines. The lines become thicker with higher gasoline consumption.

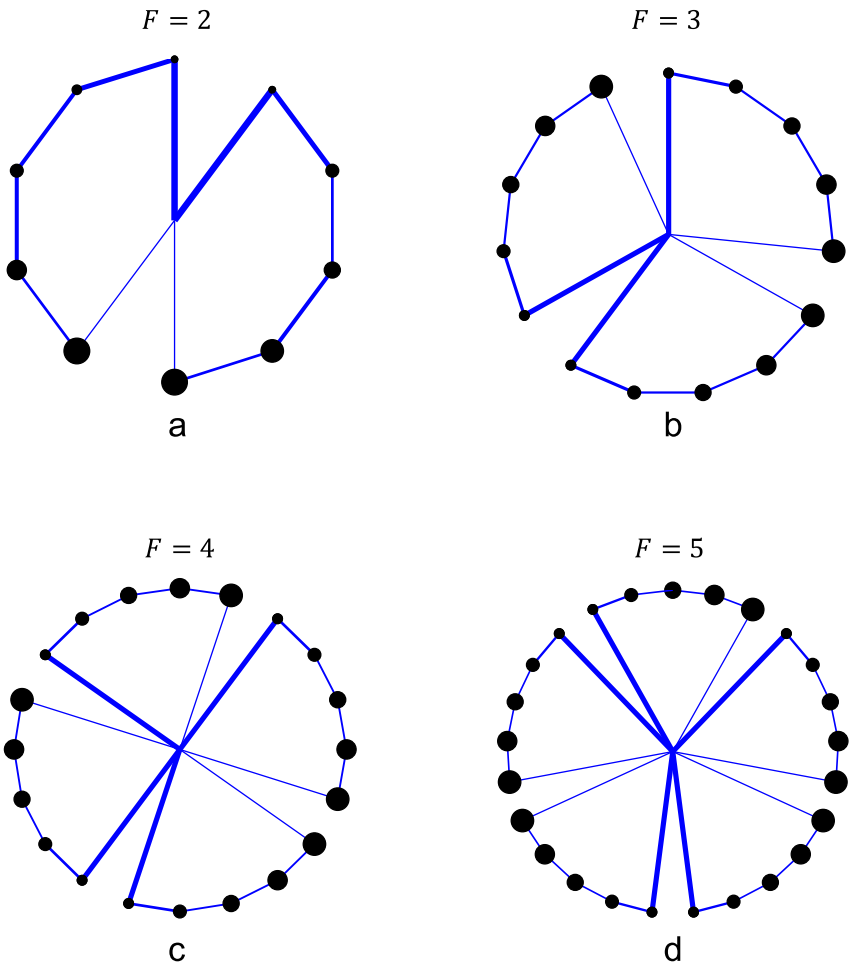

Fig. 6. PHEVRP routes in several circular networks.

5.2. Benchmarks and heuristics

We begin by testing the performance of the heuristic model on a very simplified network of Fig. 7a that has 4 directed arcs and two customers that need to be visited with one PHEV. The network has two feasible routes: Route 1, denoted by R_1, is depicted in Fig. 7b and Route 2, denoted by R_2, is depicted in Fig. 7c. For simplicity, the depot arcs (i.e., arc $0 \rightarrow 1$ and $2 \rightarrow 0$) can be traveled at no cost (i.e. gasoline and electricity consumption are zero). The other two arcs can be traveled in either all-electric or all-gasoline mode. When taking route R_1, arc $1 \rightarrow 2$ can be traveled in either all-electric mode (with A charge-units) or all-gasoline mode (with B gasoline-units). Similarly, when taking route R_2, arc $1 \rightarrow 2$ can be traveled in either all-electric mode (with C charge-units) or all-gasoline mode with (D gasoline-units) as depicted in Fig. 7a. We finally assume that

- $A > C$, so that $1 \rightarrow 2$ requires higher electricity in R_1 in all-electric mode.
- $B < D$, so that $1 \rightarrow 2$ requires more gasoline in R_2 when in all-gasoline mode.

Recall the two stages of the heuristic method. In the "route-first" stage, we choose the route with the lowest cost in all gasoline mode. Hence, the heuristic solution is to take R_1 because this route has a lower gasoline consumption since $B < D$. In the "distribute-second" stage, we need to distribute power from the two energy sources. The optimal power distribution, however, highly depends on the available battery capacity. In what follows, we compare the heuristic with the exact method at different battery capacities M. In Fig. 8, we increase the battery capacity from zero to infinity and we report the objective function (i.e., total gasoline consumption) of the two models:

- High battery capacity ($M > A$): In this case, because of the high battery capacity, the heuristic route R_1 can be traveled in all-electric mode. Hence, the total gasoline consumption of the heuristic is equal to zero. The exact method also leads to zero gasoline consumption because of sufficient battery capacity. This indicates that the two methods have the same performance with zero gasoline consumption.
- Medium battery capacity ($C < M < A$): In this case, the heuristic route R_1 must be traveled in all-gasoline mode because the vehicle does not have enough battery capacity (since $M < A$) to take the all-electric mode. Hence, the cost of the heuristic is B. The alternative route R_2, chosen by the exact method, however, can be traveled in all-electric mode because $C < M$. Hence, the cost of the exact method is zero.
- Low battery capacity ($M < C$): In this case, neither of the routes can be taken in all-electric mode because of the low battery capacity. Hence, any chosen route must be traveled in all-gasoline mode. Given that route R_1 has a lower gasoline consumption (since $B < D$) this route is chosen in both the exact and the heuristic method with a total cost of B gasoline units.

It is evident that the heuristic performs similar to the exact method when the battery capacity is either high or low. When the battery capacity is low, the vehicles drive primarily on gasoline because electricity is not available. Hence the heuristic and the exact method give the same result that can be obtained by solving a VRP with edge costs equal to the gasoline consumption. On the other hand, when the battery capacity is large, the vehicles can travel entirely in the all-electric mode. In this case, the heuristic and the exact method both have zero gasoline consumption. We present a second example in Appendix A to compare the heuristic with the exact model.

The algorithm is tested on benchmark instances retrieved from coin-or.org[1]. Series P, A, B, and E of the instances were chosen, and the power management strategies are randomly generated. All tests were performed on a laptop with four 3 GHz processors and 16 GB of RAM memory. The algorithms were coded in Matlab 2014 and solved using CPLEX 12.5 whenever a mixed-integer program or a linear program was called. In Table 1, we report the objective function and the CPU seconds of the two methods in each instance. As is shown, the cost of the exact method is strictly lower than the heuristic, but the heuristic is much faster than the exact pricing algorithm. The difference in the computation time increases with the size of the problem. We present the schematic solution of several benchmark instances in Fig. 9. Similar to previous cases, the size of the black dots represents the remaining SOC and the thickness of the blue lines represents the intensity of gasoline consumption. In all instances, it is evident that the SOC becomes smaller and tends to zero as the vehicles get closer to the depot. This indicates that the PHEVs are efficiently using their battery as they do not return to the depot with extra electric capacity that could have been used along their path to lower their gasoline consumption.

5.3. Case study of Toronto

The case study includes the Toronto financial district and the eastern part of the Toronto Waterfront as shown in Fig. 10. The depot is located at Node 0, and 15 customers are located at Nodes {2, 25, 26, 27, 19, 43, 21, 10, 30, 22, 11, 48, 13, 50, 37}. The arcs of the network are categorized into the following five groups based on speed limits and driving behaviors. The five arc types are: Freeway (average speed = 41 kph), Lake Shore Blvd. (average speed = 28.5 kph), University Ave. (average speed = 12.4 kph), Major arterial (average speed = 16.6 kph), and Major arterial with transit (average speed = 16.9 kph). The driving cycles for each link of the network is developed using the methodology proposed by Amirjamshidi and Roorda (2015). The driving cycles are used to generate the power management strategies to find the optimal PHEV routing policy. We assume that there is only one PHEV in the

[1] The exact URL of the benchmark instances is http://www.coin-or.org/symphony/branchandcut/vrp/data

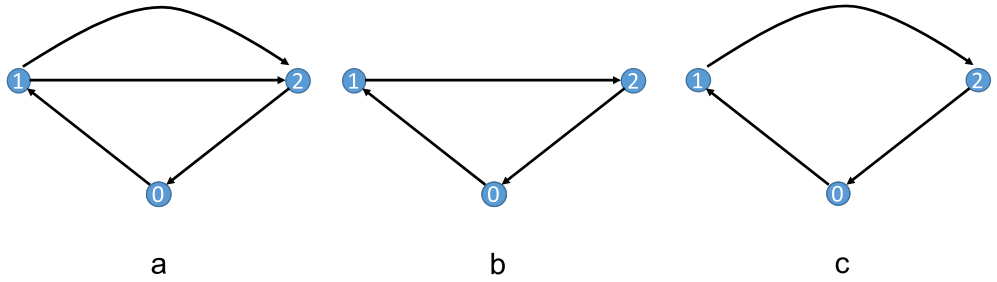

Fig. 7. (a) Hypothetical network for comparing the heuristic model with the exact pricing model, (b) First feasible route, (c) Second feasible route.

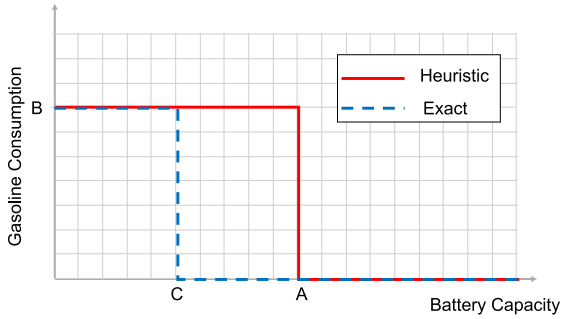

Fig. 8. Gasoline consumption at different battery capacities under the exact and heuristic algorithm.

Table 1
Comparison between the exact and heuristic algorithms on P-series benchmark instances.

Test Instance	Number of Customers	Number of Vehicles	Exact Method		Heuristic Method	
			Cost	Time (CPU Seconds)	Cost	Time (CPU Seconds)
Pn16k8	16	8	406.2	0.68	434.2	0.23
Pn19k2	19	2	197.1	1.76	221.1	0.35
Pn20k2	20	2	209.8	1.81	249.8	0.44
Pn21k2	21	2	210.6	1.79	254.9	0.51
Pn22k2	22	2	215.2	2.51	249.3	1.34
Pn22k8	22	8	450.3	2.35	475.6	1.24
Pn23k8	23	8	384.7	2.71	410.5	1.65
Pn40k5	40	5	440.2	26.3	477.6	9.5
Pn45k5	45	5	462.1	27.2	483.8	15.7
Pn50k7	50	7	499.2	41.3	511.5	19.6
Pn50k8	50	8	525.2	56.95	564.2	22.7
Pn50k10	50	10	583.7	213.1	601.4	39.9
An32k5	32	5	845.4	150.7	983.7	43.8
An37k5	37	5	903.9	85.5	1329.5	32.4
Bn41k6	41	6	1302.4	469.2	1536.4	293.5
Bn50k8	50	8	1560.3	895.3	1844.3	348.5
En13k4	13	4	438.4	0.52	573.5	0.19

network that has to visit all 15 customers.

We consider three vehicle types; the electric driving range of the vehicles is 35 km, 25 km, and 15 km. Fig. 11a depicts the SOC profile when a charger is located at customer 10. We observe a distinct power consumption pattern for each vehicle. The long-range PHEV (35 km) has an overall even electricity consumption along its path; especially in the first 7 km of the path where electricity consumption is roughly constant for PHEV-35. The other two vehicles, however, consume more gasoline on the highways, thus allowing them to preserve more electricity to travel between the customers where a lot of idling is required due to higher traffic in this region. Fig. 11a also shows that all vehicles consume their entire electricity at the end of the path, which allows them to consume less gasoline along the entire path. Furthermore, the increase in the SOC in the middle of the path is due to charging at customer 10.

We also test a scenario without any chargers. The SOC profiles of the vehicles are presented in Fig. 11b. The two lower range vehicles, PHEV-25 and PHEV-15, consume all electricity before ending the path. The long-range vehicle, PEHV-35, however, is able to preserve more electricity due to the larger battery size. Evidently, the absence of the charger leads to an overall larger gasoline consumption for all three vehicle types. The gasoline consumption increases by 8%, 11%, and 15% for the longest to the lowest range PHEVs. This confirms the intuition that chargers are more impactful when the PHEV fleet has a smaller electric driving range. The

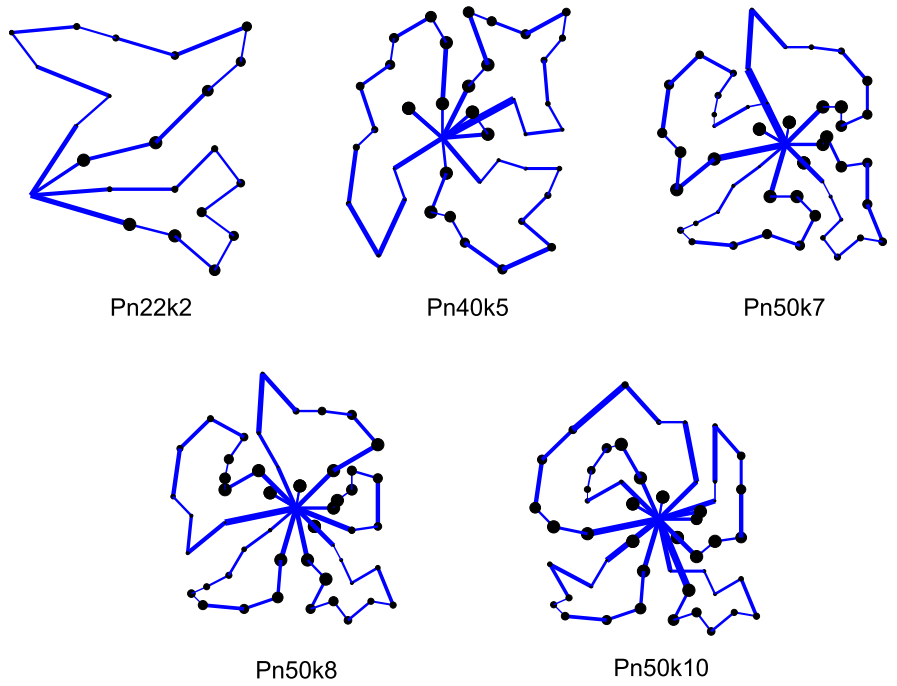

Fig. 9. Graphical representation of selected benchmark instances.

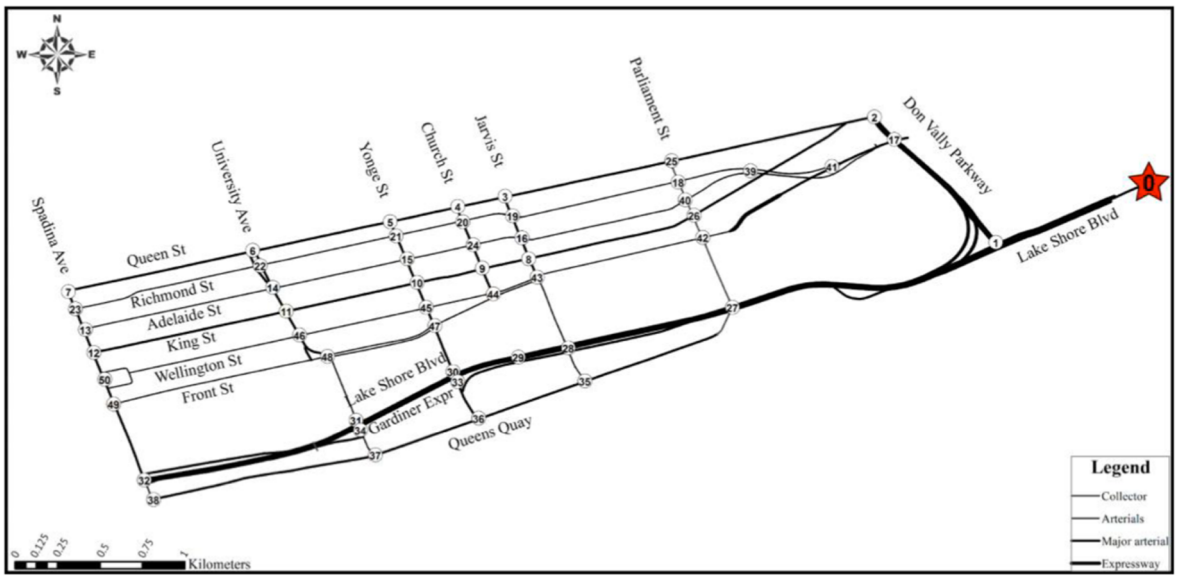

Fig. 10. Toronto Waterfront network with 5 different link types.

chargers play the role of virtually increasing the driving range for these vehicles.

For the case study of the City of Toronto, we have used the heuristic algorithm with a maximum time limit of 5 min. Although the number of customers is small in the case study, the problem is still difficult to solve due to the large number of power management strategies for traversing each of the links of the network. Further discussion of the computation complexity is presented in Table 1.

6. Conclusions

Growing concerns over increasing GHG emissions and petroleum dependency have enticed a stream of new policies for using alternative fuel vehicles in commercial fleets. Among them, PHEVs and electric vehicles are environmentally friendly and meet the required regulations. Despite their benefits, electric vehicles cause range anxiety due to low battery capacities. In contrast PHEVs

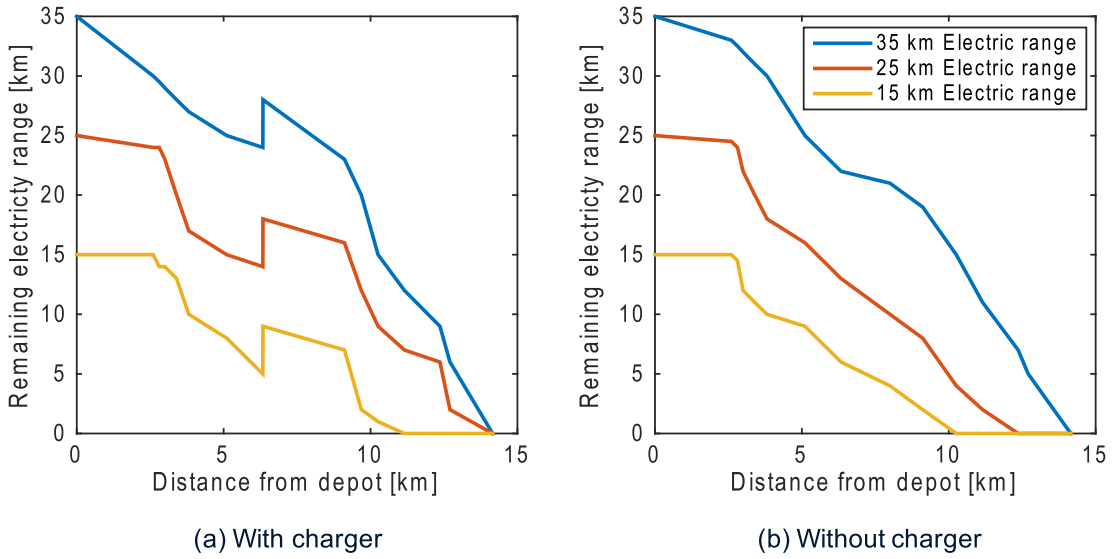

Fig. 11. State of charge profile of three PHEVs along their path in the Toronto Waterfront network.

satisfy regulations without any range anxiety issues. This paper presents a PHEV routing model that is solved using an exact and a heuristic algorithm. We derive the computation time order of each algorithm and show that the heuristic becomes substantially faster as the size of the PHEV battery increases. Moreover, we show that the heuristic performs as well as the exact method when the PHEV battery is either very small or very large. In mid-range batteries, however, the exact method provides a better objective function than the heuristic at the cost of a longer computation time.

The presented PHEVRP model can be extended in several ways. First, we did not account for regenerative braking to keep the model simple. Although regenerative braking may not substantially alter the results, accounting for it improves the accuracy of the model. Second, our power management model is static and offline and thus solved using dynamic programming. In reality, however, we need to consider a wide range of possible driving cycles on each arc of the network. Finally, application of the PHEVRP in a fleet composition model can help find the optimal mix of vehicles types including electric vehicles, PHEVs, and internal combustion engine vehicles.

Appendix A:. Comparing the heuristic to the exact

We present a second example here to compare the heuristic with the exact method. Consider the network presents in Fig. 12a that has 6 directed arcs, 1 bi-directional arc, and 4 customers that need to be visited by one PHEV. All arcs can be traveled at no cost (i.e. gasoline and electricity consumption is zero) except for the following arcs: Arc $1 \rightarrow 2$needs A charge units and B gasoline units; Arc $1 \rightarrow 3$needs D charge units and E gasoline units. The network is symmetric such that arcs $1 \rightarrow 3$ is identical to $2 \rightarrow 4$ and arc $1 \rightarrow 2$ is identical to $3 \rightarrow 4$. This example is set up so that there are two feasible traveling salesman routes for visiting all customers with one PHEV. The first feasible tour is shown in Fig. 12b that requires 2A charge units and 2B gasoline units. The second feasible tour is shown in Fig. 12c that needs 2C charge units and 2E gasoline units.

Finally, we assume that

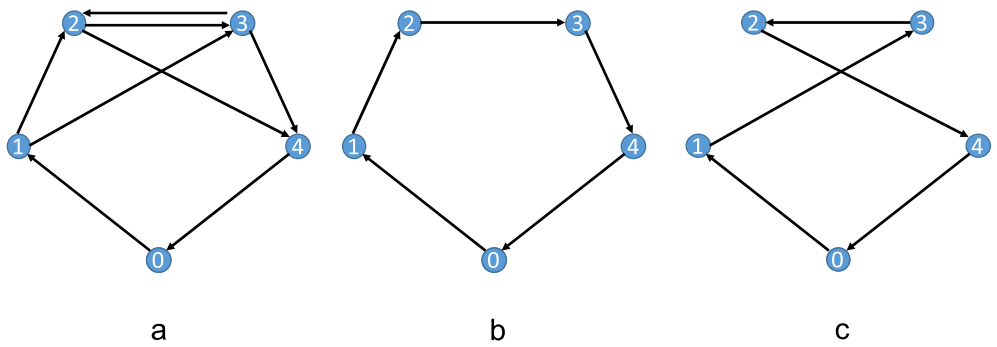

Fig. 12. (a) Hypothetical network for comparing the heuristic model with the exact pricing model, (b) First feasible route, (c) Second feasible route.

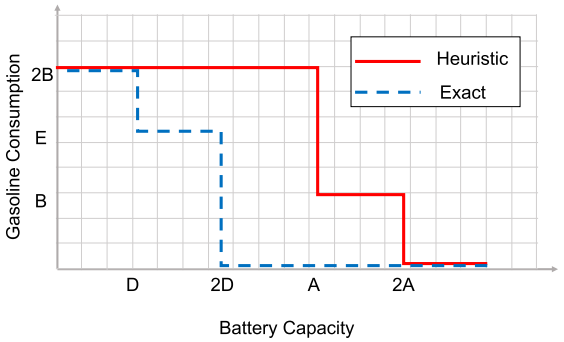

Fig. 13. Gasoline consumption at different battery capacities under the exact and heuristic algorithm.

- $A > 2D$, so that $1 \rightarrow 2$ needs higher electricity than $1 \rightarrow 3$, and
- $2B < E$, so that $1 \rightarrow 2$ needs less gasoline than $1 \rightarrow 3$.

Let us now compare the heuristic and the exact model at different battery capacities M. In Fig. 13, we increase the battery capacity from zero to infinity and we report the objective function (i.e., total gasoline consumption) of the two models.

- Low battery capacity ($M < 2D$): In this case, the two models have the same performance and have the route presented in Fig. 7b.
- High battery capacity ($M > 2A$): In this case, the two models have the same performance, and both have the route presented in Fig. 7c.
- Medium battery capacity ($2D < M < 2A$): In this case, the exact model always performs better than the heuristic model.

The presented example shows that the heuristic and the exact have the same performance when the battery capacity is either large or small. In other instances, the exact performs better than that heuristic in terms of the total gasoline consumption.

References

Abdallah, T., 2013. The plug-in hybrid electric vehicle routing problem with time windows. UWSpace.
Amirjamshidi, G., Roorda, M.J., 2015. Development of simulated driving cycles for light, medium, and heavy duty trucks: Case of the Toronto Waterfront Area. Transport. Res. Part D: Transport Environ. 34, 255–266.
Bektaş, T., Laporte, G., 2011. The pollution-routing problem. Transport. Res. Part B: Methodol. 45 (8), 1232–1250.
Bruglieri, M., Mancini, S., Pisacane, O., 2019. More efficient formulations and valid inequalities for the Green Vehicle Routing Problem. Transport. Res. Part C: Emerging Technol. 105, 283–296.
Chen, Z., Mi, C.C., Xu, J., Gong, X., You, C., 2014. Energy management for a power-split plug-in hybrid electric vehicle based on dynamic programming and neural networks. IEEE Trans. Veh. Technol. 63 (4), 1567–1580.
Conrad, R.G., Figliozzi, M.A., 2011. The recharging vehicle routing problem. In: IIE Annual Conference. Proceedings. Institute of Industrial Engineers-Publisher, pp. 1.
Davis, B.A., Figliozzi, M.A., 2013. A methodology to evaluate the competitiveness of electric delivery trucks. Transport. Res. Part E: Logistics Transport. Rev. 49 (1), 8–23.
Deflorio, F., Castello, L., 2017. Dynamic charging-while-driving systems for freight delivery services with electric vehicles: Traffic and energy modelling. Transport. Res. Part C: Emerging Technol In press.
Demir, E., Bektaş, T., Laporte, G., 2014. The bi-objective pollution-routing problem. Eur. J. Oper. Res. 232 (3), 464–478.
Dekker, R., Bloemhof, J., Mallidis, I., 2012. Operations Research for green logistics–An overview of aspects, issues, contributions and challenges. Eur. J. Operat. Res. 219 (3), 671–679. https://doi.org/10.1016/j.ejor.2011.11.010.
Demir, E., Bektaş, T., Laporte, G., 2012. An adaptive large neighborhood search heuristic for the pollution-routing problem. Eur. J. Oper. Res. 223 (2), 346–359.
Eksioglu, B., Vural, A.V., Reisman, A., 2009. The vehicle routing problem: A taxonomic review. Comput. Ind. Eng. 57 (4), 1472–1483.
Electrification Coalition. 2015. Electrification Roadmap: Revolutionizing transportation and achieving energy security.
Erdoğan, S., Miller-Hooks, E., 2012. A green vehicle routing problem. Transport. Res. Part E: Logistics Transport. Rev. 48 (1), 100–114.
Figliozzi, M., 2010. Vehicle routing problem for emissions minimization. Transport. Res. Record: J. Transporta. Res. Board 2197, 1–7.
Franceschetti, A., Honhon, D., Van Woensel, T., Bektaş, T., Laporte, G., 2013. The time-dependent pollution-routing problem. Transport. Res. Part B: Methodol. 56, 265–293.
Fukasawa, R., He, Q., Song, Y., 2015. A branch-cut-and-price algorithm for the energy minimization vehicle routing problem. Transport. Sci. 50 (1), 23–34.
Fukasawa, R., Longo, H., Lysgaard, J., de Aragão, M.P., Reis, M., Uchoa, E., Werneck, R.F., 2006. Robust branch-and-cut-and-price for the capacitated vehicle routing problem. Math. Program. 106 (3), 491–511.
Gonçalves, F., Cardoso, S.R., Relvas, S., Barbosa-Póvoa, A.P.F.D. (2011). Optimization of a distribution network using electric vehicles: A VRP problem. In: Proceedings of the IO2011-15 Congresso da associação Portuguesa de Investigação Operacional, Coimbra, Portugal. pp. 18–20.
He, Y., Chowdhury, M., Pisu, P., Ma, Y., 2012. An energy optimization strategy for power-split drivetrain plug-in hybrid electric vehicles. Transport. Res. Part C: Emerging Technol. 22, 29–41.
Hiermann, G., Hartl, R.F., Puchinger, J., Vidal, T., 2019. Routing a mix of conventional, plug-in hybrid, and electric vehicles. Eur. J. Oper. Res. 272 (1), 235–248.
Jabali, O., Woensel, T., de Kok, A.G., 2012. Analysis of travel times and CO2 emissions in time-dependent vehicle routing. Prod. Operations Manage. 21 (6), 1060–1074.
Koç, Ç., Bektaş, T., Jabali, O., Laporte, G., 2014. The fleet size and mix pollution-routing problem. Transport. Res. Part B: Methodol. 70, 239–254.
Kolmanovsky, I.V., Lezhnev, L., Maizenberg, T.L., 2008. Discrete-time drift counteraction stochastic optimal control: theory and application-motivated examples. Automatica 44 (1), 177–184.
Kopfer, H.W., Schönberger, J., Kopfer, H., 2014. Reducing greenhouse gas emissions of a heterogeneous vehicle fleet. Flexible Serv. Manuf. J. 26 (1–2), 221–248.

Kwon, Y.J., Choi, Y.J., Lee, D.H., 2013. Heterogeneous fixed fleet vehicle routing considering carbon emission. Transport. Res. Part D: Transport Environ. 23, 81–89.
Mancini, S., 2017. The hybrid vehicle routing problem. Transport. Res. Part C: Emerging Technol. 78, 1–12.
McKinnon, A. 2010. Environmental sustainability. Green logistics: improving the environmental sustainability of logistics. London.
Oh, K., Min, J., Choi, D., Kim, H., 2007. Optimization of control strategy for a single-shaft parallel hybrid electric vehicle. Proc. Institut. Mech. Eng., Part D: J. Automob. Eng. 221 (5), 555–565.
Pillac, V., Gendreau, M., Guéret, C., Medaglia, A.L., 2013. A review of dynamic vehicle routing problems. Eur. J. Oper. Res. 225 (1), 1–11.
Raykin, L., Roorda, M.J., MacLean, H.L., 2012. Impacts of driving patterns on tank-to-wheel energy use of plug-in hybrid electric vehicles. Transport. Res. Part D: Transport Environ. 17 (3), 243–250.
Qi, X., Luo, Y., Wu, G., Boriboonsomsin, K., Barth, M., 2019. Deep reinforcement learning enabled self-learning control for energy efficient driving. Transport. Res. Part C: Emerging Technol. 99, 67–81.
Ribau, J., Viegas, R., Angelino, A., Moutinho, A., Silva, C., 2014a. A new offline optimization approach for designing a fuel cell hybrid bus. Transport. Res. Part C: Emerging Technol. 42, 14–27.
Ribau, J.P., Silva, C.M., Sousa, J.M., 2014b. Efficiency, cost and life cycle CO 2 optimization of fuel cell hybrid and plug-in hybrid urban buses. Appl. Energy 129, 320–335.
Sampathnarayanan, B., Onori, S., Yurkovich, S., 2014. An optimal regulation strategy with disturbance rejection for energy management of hybrid electric vehicles. Automatica 50 (1), 128–140.
Schneider, M., Stenger, A., Goeke, D., 2014. The electric vehicle-routing problem with time windows and recharging stations. Transport. Sci. 48 (4), 500–520. https://doi.org/10.1287/trsc.2013.0490.
Sinoquet, D., Rousseau, G., Milhau, Y., 2011. Design optimization and optimal control for hybrid vehicles. Optimiz. Eng. 12 (1), 199–213.
Toth, P., Vigo, D. (Eds.), 2014. Vehicle routing: problems, methods, and applications. Society for Industrial and Applied Mathematics.
Uchoa, E., 2011. Cuts over extended formulations by flow discretization. Prog. Combinatorial Optimiz. 255–282.
US DOE. 2010. Transportation Data Book, In: Davis, S.C., Diegel, S.W., Boundy, R.G. (Eds.), 29th ed. Oak Ridge National Laboratory. ORNL, 6985.
US FHWA, Federal Highway Administration, 2008. Highway Statistics 2008. < http://www.fhwa.dot.gov/policyinformation/statistics/2008/vm1.cfm > Accessed Feb 2, 2016.
Yao, J., Moawad, A., 2019. Vehicle energy consumption estimation using large scale simulations and machine learning methods. Transport. Res. Part C: Emerging Technol. 101, 276–296.
Zhang, C., Vahidi, A., Li, X., Essenmacher, D., 2009. Role of trip information preview in fuel economy of plug-in hybrid vehicles. In: *ASME 2009 dynamic systems and control conference*. American Society of Mechanical Engineers, pp. 253–258.
Zhang, P., Yan, F., Du, C., 2015. A comprehensive analysis of energy management strategies for hybrid electric vehicles based on bibliometrics. Renew. Sustain. Energy Rev. 48, 88–104.